Interaction Mechanisms between Polyamines and IRK1 Inward Rectifier K^+ Channels

Donglin Guo and Zhe Lu

Department of Physiology, University of Pennsylvania, Philadelphia, PA 19104

ABSTRACT Rectification of macroscopic current through inward-rectifier K^+ (Kir) channels reflects strong voltage dependence of channel block by intracellular cations such as polyamines. The voltage dependence results primarily from the movement of K^+ ions across the transmembrane electric field, which accompanies the binding–unbinding of a blocker. Residues D172, E224, and E299 in IRK1 are critical for high-affinity binding of blockers. D172 appears to be located somewhat internal to the narrow K^+ selectivity filter, whereas E224 and E299 form a ring at a more intracellular site. Using a series of alkyl-bis-amines of varying length as calibration, we investigated how the acidic residues in IRK1 interact with amine groups in the natural polyamines (putrescine, spermidine, and spermine) that cause rectification in cells. To block the pore, the leading amine of bis-amines of increasing length penetrates ever deeper into the pore toward D172, while the trailing amine in every bis-amine binds near a more intracellular site and interacts with E224 and E299. The leading amine in nonamethylene-bis-amine (bis-C9) makes the closest approach to D172, displacing the maximal number of K^+ ions and exhibiting the strongest voltage dependence. Cells do not synthesize bis-amines longer than putrescine (bis-C4) but generate the polyamines spermidine and spermine by attaching an amino-propyl group to one or both ends of putrescine. Voltage dependence of channel block by the tetra-amine spermine is comparable to that of block by the bis-amines bis-C9 (shorter) or bis-C12 (equally long), but spermine binds to IRK1 with much higher affinity than either bis-amine does. Thus, counterintuitively, the multiple amines in spermine primarily confer the high affinity but not the strong voltage dependence of channel block. Tetravalent spermine achieves a stronger interaction with the pore by effectively behaving like a pair of tethered divalent cations, two amine groups in its leading half interacting primarily with D172, whereas the other two in the trailing half interact primarily with E224 and E299. Thus, nature has optimized not only the blocker but also, in a complementary manner, the channel for producing rapid, high-affinity, and strongly voltage-dependent channel block, giving rise to exceedingly sharp rectification.

KEY WORDS: Kir • polyamine • alkyl-bis-amine • block • voltage dependence

INTRODUCTION

Inward-rectifier K^+ (Kir) channels conduct much larger inward K^+ currents at membrane voltages (V_m) negative to the K^+ equilibrium potential (E_K) than outward currents at V_m positive to E_K, even when K^+ concentrations on both sides of the membrane are made equal (Katz, 1949; Hodgkin and Horowicz, 1959; Noble, 1962, 1965; Hagiwara and Takahashi, 1974; Hagiwara et al., 1976). This unusual conduction property, referred to as anomalous or inward rectification, underlies the ability of Kir to accomplish many important biological tasks.

The first clue to the functions of inwardly rectifying K^+ currents came from the studies by Noble (1962, 1965) of cardiac Purkinje fibers, where he hypothesized that potassium conductance decreases upon membrane depolarization and thus helps produce the long plateau phase in the action potential, and then increases during membrane repolarization, accelerating the descending phase. On the other hand, the first clue to a possible mechanism came from the work of Armstrong and Binstock (1965), who showed that intracellular TEA blocks voltage-activated K^+ channels of squid axon in a voltage-dependent manner, rendering them inwardly rectifying.

Two decades later, Mg^{2+} was identified as an endogenous voltage-dependent channel blocker causing inward rectification (Matsuda et al., 1987; Vandenberg, 1987). However, voltage dependence of Mg^{2+} (or TEA) block is too weak to account for the sharp inward rectification observed in many cell types. Moreover, significant inward rectification persisted in the nominal absence of Mg^{2+}. Therefore, the possibility remained that inward rectification results from intrinsic channel gating (e.g., Kurachi, 1985; Ishihara et al., 1989; Silver and DeCoursey, 1990; Stanfield et al., 1994a). There was little progress in the search for additional causes of rectification until the intracellular polyamines putrescine

Address correspondence to Dr. Zhe Lu, University of Pennsylvania, Department of Physiology D302A Richards Building, 3700 Hamilton Walk, Philadelphia, PA 19104. Fax: (215) 573-1940; email: zhelu@mail.med.upenn.edu

Abbreviations used in this paper: PUT, putrescine; SPD, spermidine; SPM, spermine.

(PUT), spermidine (SPD), and spermine (SPM) (see Fig. 18 A for structures) were found to block the channels in a strongly voltage-dependent manner (Ficker et al., 1994; Lopatin et al., 1994; Fakler et al., 1995). The apparent valences of steady-state channel block by spermidine and spermine are approximately five (Guo and Lu, 2000b,c), sufficiently large to account for the sharp rectification observed in cells. Lowering the concentration of intracellular polyamines reduces the extent of rectification (Bianchi et al., 1996; Shyng et al., 1996; Lopatin et al., 2000). Furthermore, in the absence of intracellular blockers, the steady-state macroscopic I-V curve of wild-type IRK1 channels is practically linear (Guo and Lu, 2000c, 2002). Together, these findings indicate that inward rectification in IRK1 channels indeed reflects the strong voltage dependence of channel block.

Cloning of Kir channels enabled their molecular characterization (Ho et al., 1993; Kubo et al., 1993). For high-affinity binding of cationic blockers, an acidic residue (e.g., D172 in IRK1) within the second transmembrane (M2) segment of Kir channels is crucial (Lu and MacKinnon, 1994; Stanfield et al., 1994b; Wible et al., 1994). In ROMK1 (Kir1.1), an acidic residue substituted at the corresponding position (171) in M2 confers a much higher affinity for blocking ions, while a basic residue renders the channel essentially insensitive. On the basis of these findings, it was proposed that residue 171 affects the binding of blocking ions through an electrostatic mechanism (Lu and MacKinnon, 1994), a proposal further supported by the fact that the presence of Asp at any of a number of sites in M2 enhances rectification (Guo et al., 2003). Addition-

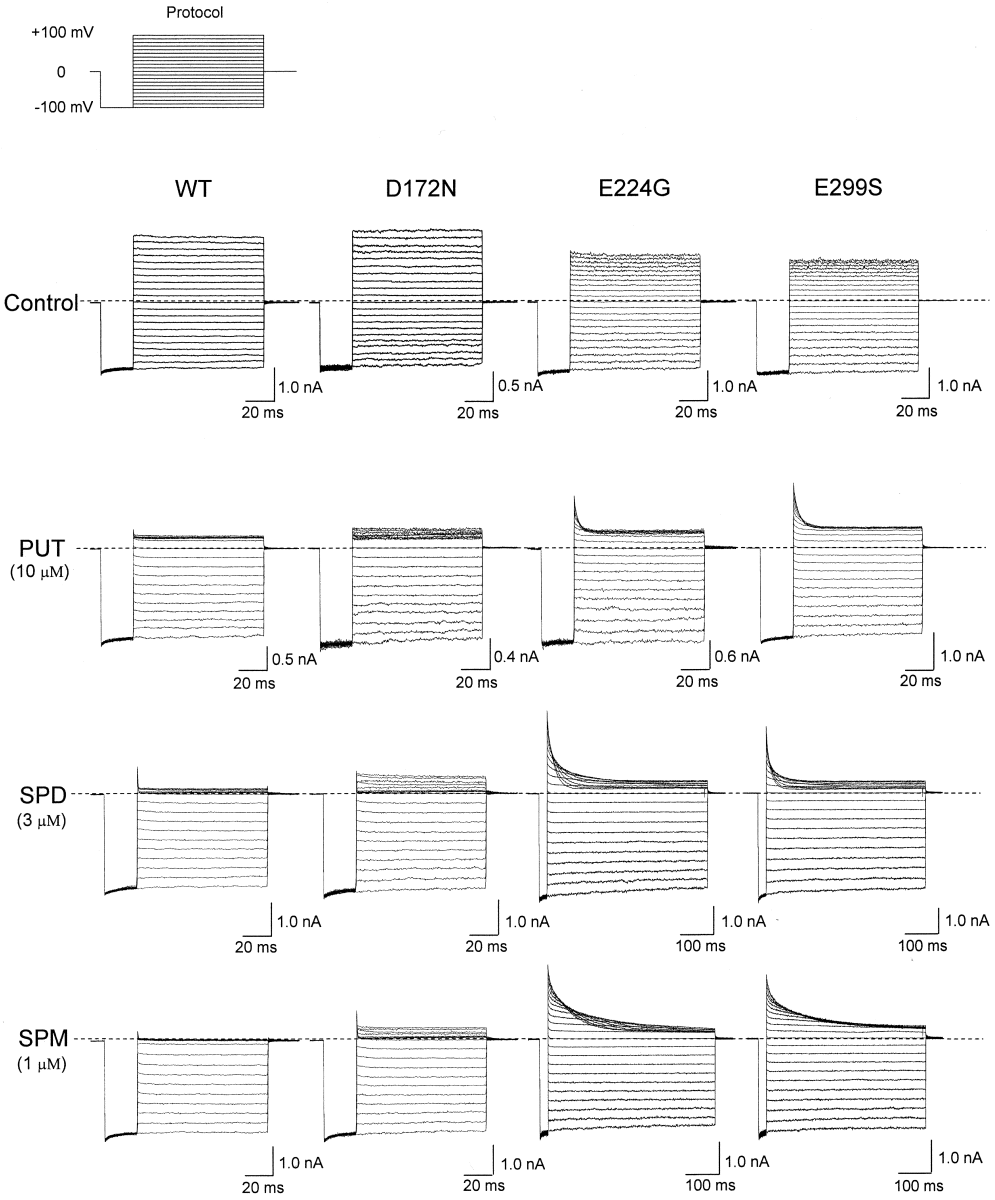

FIGURE 1. Effects of single mutations within M2 or the COOH terminus on current inhibition by polyamines. Shown are currents of wild-type and mutant channels containing a single mutation, D172N, E224G, or E299S, recorded from various patches in the absence (control) or presence of PUT, SPD, or SPM at concentrations indicated, and with the voltage protocol shown at the top. Dashed lines identify zero current levels.

ally, substituting a neutral residue for certain acidic residues (E224 and E299) in the COOH terminus of IRK1 (Kir2.1) has been shown to affect channel block by intracellular blockers (Taglialatela et al., 1994, 1995; Yang et al., 1995; Kubo and Murata, 2001), which suggests that the COOH terminus extends the pore intracellularly beyond what is formed by M2.

Determination of atomic structures of various K^+ channels dramatically advanced our understanding of their structure-function relationship. Studies on the KcsA pore show how the K^+ selectivity filter (~12 Å long) is formed by the signature sequence within the region between M1 and M2, while the remaining, internal part of the pore (~20 Å) is lined by M2, and also how the structure gives rise to K^+ conduction (Doyle et al., 1998; Morais-Cabral et al., 2001; Zhou et al., 2001). Studies on the cytoplasmic termini of GIRK1 (Kir3.1) show how they form a structure extending the pore intracellularly by at least another ~30 Å beyond what is formed by M2 (Nishida and MacKinnon, 2002). The middle part of the pore extension is wide while both ends are relatively narrow, ranging from 7 to 15 Å. This inner pore extension is thus sufficiently wide to accommodate hydrated K^+ ions, although their presence there, or that of any blocking ions, remains to be demonstrated. Furthermore, the structure of a bacterial Kir (KirBac1.1) shows that the length of the entire channel pore is ~90 Å, and reveals how the two parts of the inner pore, formed by M2 and the COOH terminus, are connected (Kuo et al., 2003). The residue corresponding to D172 in IRK1 is located somewhat internal to the K^+ selectivity filter, while those corresponding to E224 and E299 in IRK1 form a ring in the inner pore extension (Nishida and MacKinnon, 2002; Kuo et al., 2003). Based on the structure of KirBac1.1, the distance between the acidic residues in M2 and those in the COOH terminus of IRK1 is ~35 Å (Kuo et al., 2003), significantly greater than the length of a natural polyamine molecule (≤20 Å).

A systematic functional study of the interaction energy between a series of alkyl-bis-amines (bis-amines) of varying length and D172 in M2 or E224 and E299 in the COOH terminus of IRK1 shows that, while the leading amine group extends further outward toward D172 as alkyl chain length is increased, the trailing amine group in all bis-amines binds near the same intracellular site independent of chain length (Guo et al., 2003). The leading amine group in nonamethylene-bis-amine (bis-C9) comes closest to D172, with ~2 kcal/mol interaction energy. On the other hand, the interaction energy is more modest (<1 kcal/mol) between the trailing amine group and E224/E299 located more intracellularly, consistent with the latter interaction occurring over a greater distance. The apparent voltage dependence of channel block reflects primarily the movement of K^+ ions, not of blockers, across the transmembrane electric field, because the degree of voltage dependence correlates not with the number of positive charges carried by amine blockers but with their length. That is, the apparent valence of channel block by alkyl-mono-amines (mono-amines) or bis-amines that carry maximally one or two charges increases to four to five with increasing blocker length. These studies form a basis for addressing the critical issue of how the acidic residues in the chan-

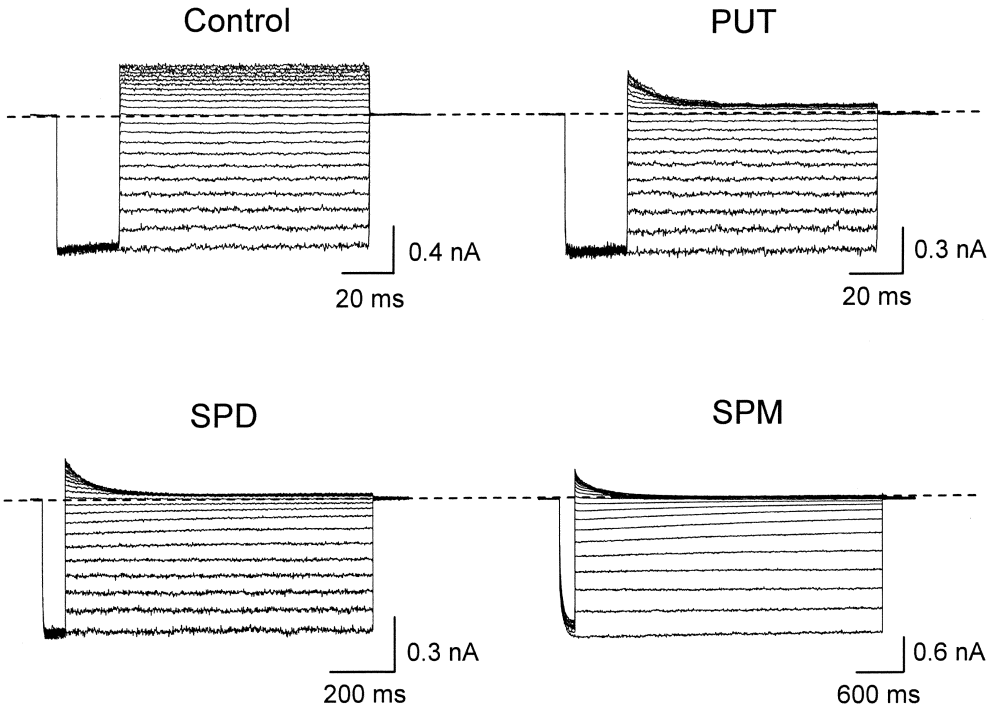

FIGURE 2. Polyamine inhibition of currents of IRK1 with a double mutation in the COOH terminus. Shown are currents of mutant channels containing the double mutation E224G+E299S recorded from various patches in the absence (control) or presence of 0.3 mM PUT, SPD, or SPM. Dashed lines identify zero current levels.

nel interact with the individual amine groups in the three natural polyamines PUT, SPD, and SPM.

MATERIALS AND METHODS

Molecular Biology and Oocyte Preparation

The cDNA of IRK1 (Kubo et al., 1993) was subcloned in pGEM-HESS plasmid (Liman et al., 1992). All mutant cDNAs were obtained through PCR-based mutagenesis and confirmed by DNA sequencing. The cRNAs were synthesized with T7 polymerase (Promega Corp.) using linearized cDNAs as templates. Oocytes harvested from *Xenopus laevis* (*Xenopus* One) were incubated in a solution containing NaCl, 82.5 mM; KCl, 2.5 mM; $MgCl_2$, 1.0 mM; HEPES (pH 7.6), 5.0 mM; and collagenase, 2–4 mg/ml. The oocyte preparation was agitated at 80 rpm for 60–90 min. It was then rinsed thoroughly and stored in a solution containing NaCl, 96 mM; KCl, 2.5 mM; $CaCl_2$, 1.8 mM; $MgCl_2$, 1.0 mM; HEPES (pH 7.6), 5 mM and gentamicin, 50 μg/ml. Defolliculated oocytes were selected and injected with RNA at least 2 and 16 h, respectively, after collagenase treatment. All oocytes were stored at 18°C.

Recordings and Solutions

Macroscopic currents were recorded from inside-out membrane patches of *Xenopus* oocytes heterologously expressing either wild-type or mutant IRK1 channels using an Axopatch 200B amplifier (Axon Instruments, Inc.), filtered at 5 kHz, and sampled at 25 kHz using an analogue-to-digital converter (Digidata 1322A; Axon Instruments, Inc.) interfaced with a personal computer. pClamp8 software was used to control the amplifier and acquire the data. During current recording, the voltage across the membrane patch was first hyperpolarized from the 0 mV holding potential to −100 mV, and then stepped to various test voltages between −100 and 100 mV and back to 0 mV. Background leak current correction was performed as previously described (Lu and MacKinnon, 1994; Guo and Lu, 2000c). The intracellular solution contained (mM): 5 K_2EDTA, 10 "K_2HPO_4 + KH_2PO_4" in a ratio yielding pH 8.0, and sufficient KCl to bring total K^+ concentration to 100 mM, whereas in the extracellular solution 5 mM EDTA was replaced by 0.3 mM $CaCl_2$ and 1 mM $MgCl_2$ (Guo and Lu, 2000c, 2002). All chemicals were purchased from Fluka Chemical Corp.

RESULTS

Steady-state Block of Wild-type and Mutant Channels by Natural Polyamines

As discussed in INTRODUCTION, substitution of a neutral residue for D172 in M2 and E224 or E299 in the COOH terminus has been shown to affect channel

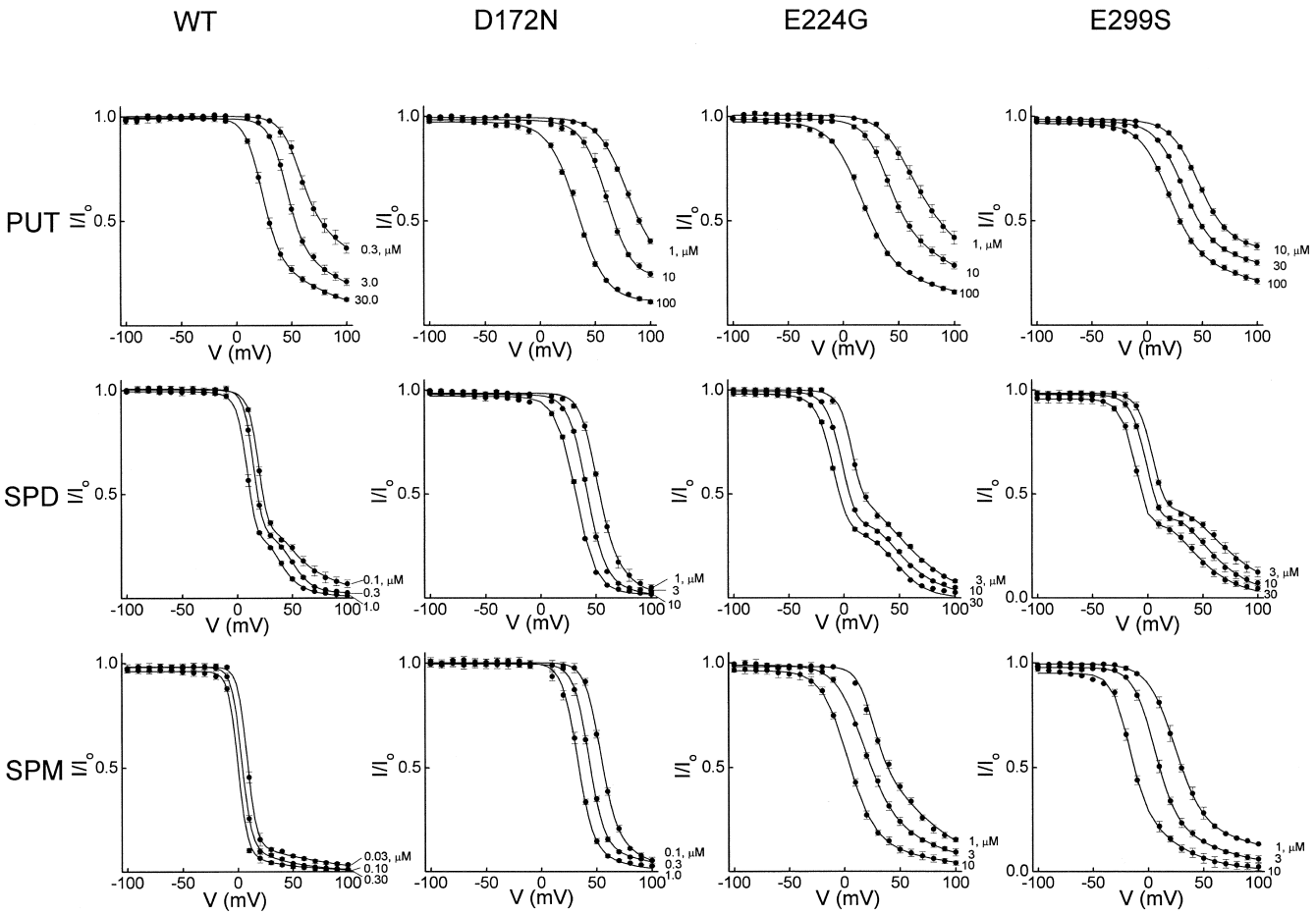

FIGURE 3. Effects of single mutations within M2 or the COOH terminus on the voltage-dependent block of IRK1 current by polyamines. The fraction of wild-type and mutant channel currents (mean ± SEM; n = 4–6) not blocked by PUT, SPD, or SPM (at the concentrations indicated) is plotted against membrane voltage. The curves fitted to the data are described in RESULTS.

block by the polyamines PUT, SPD, and SPM. Here we examine how the various amine groups in each polyamine species interact with those acidic residues in the channel pore. Fig. 1 shows current traces of wild-type and three mutant IRK1 channels recorded in the absence and presence of PUT, SPD, and SPM (for structures see Fig. 18 A). To a different extent, the three mutations reduce channel affinity for polymines, but only mutations E224G and E299S, not D172N, dramatically reduce the rate of current inhibition. Current records of channels with double mutation E224G+E299S are shown in Fig. 2. Channels containing the double mutation exhibit lower affinity for polyamines and a much slower inhibition rate. Note that replacing either E224 or E299, or both, with neutral residues renders channels inwardly rectifying in the nominal absence of any blockers (Figs. 1 and 2).

The fraction of current not blocked (I/I_o) in wild-type and mutant channels is plotted against membrane voltage (V_m) in Figs. 3 and 4 for three appropriately chosen concentrations of each amine blocker. Since PUT not only blocks the pore but also permeates with finite probability, to determine the dissociation constant (K_d) and valence (Z) of PUT we fitted the blocking curve with Eq. 1 (rewritten from Eq. 2 of Guo and Lu, 2000b),

$$\frac{I}{I_o} = \frac{1}{1 + \dfrac{[AM]}{K_d e^{-\frac{ZFV_m}{RT}}\left(1 + Pe^{\frac{Z_pFV_m}{RT}}\right)}}, \qquad (1)$$

where P is the probability of a bound blocker permeating the pore versus returning to the intracellular solution. Quantities F, R, and T have their usual meaning. As to the blocking curves for SPD or SPM, they exhibit two descending phases with an intervening hump. The two blocking phases reflect channel block by fully and partially protonated SPD or SPM (Guo and Lu, 2000a,b). In the present study, we mainly focus on examining quantitatively the behaviors of fully protonated species. To determine both K_d and Z we fitted the blocking curves for SPD and SPM with Eq. 2 (rewritten from Eq. 6 of Guo and Lu, 2000b),

$$\frac{I}{I_o} = \frac{1}{1 + [AM]\left(\dfrac{1}{K_d e^{-\frac{ZFV_m}{RT}}\left(1 + Pe^{\frac{Z_pFV_m}{RT}}\right)} + \dfrac{1}{K_d^* e^{-\frac{Z^*FV_m}{RT}}\left(1 + P^* e^{\frac{Z_p^*FV_m}{RT}}\right)}\right)} \qquad (2)$$

where all quantities are as defined for Eq. 1; "*" identifies those for the partially protonated state.

Fig. 5 summarizes K_d (0 mV) values for each polyamine in wild-type and various mutant channels and the associated valences (Z) obtained from the fits. Mutation D172N reduces the channel affinity for PUT, SPD, and SPM by ~2-, 45-, and 350-fold, respectively. On the other hand, either E224G or E299S reduces the channel affinity by about twofold for PUT and SPD but ~20-fold for SPM. Generally, effects of the two COOH-terminal mutations on amine block are comparable. Substituting a neutral residue for the acidic residues also reduces the apparent valence of channel block by SPD and SPM (but not by PUT; see below). Double mu-

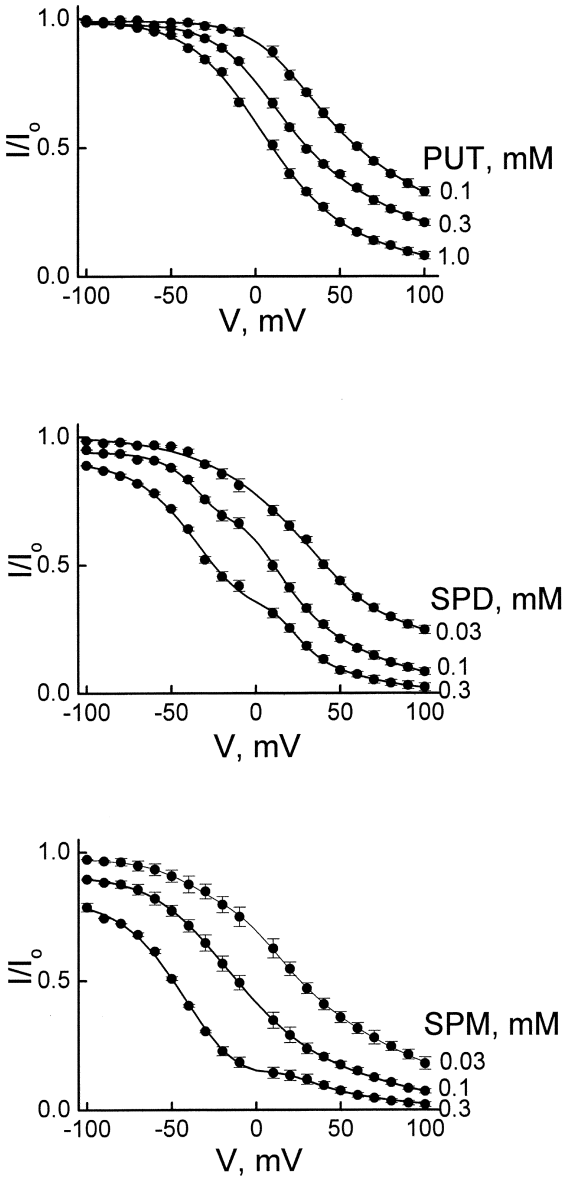

FIGURE 4. Effects of a double mutation (E224G+E299S) in the COOH terminus on the voltage-dependent block of IRK1 current by polyamines. The fraction of mutant channel currents (mean ± SEM; n = 4–6) not blocked by PUT, SPD, or SPM (at the concentrations indicated) is plotted against membrane voltage. The curves fitted to the data are described in RESULTS.

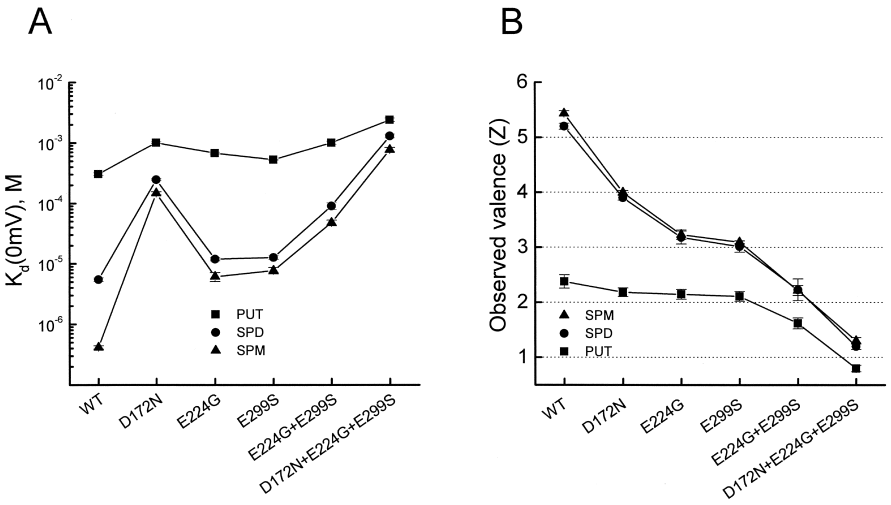

FIGURE 5. Summary of dissociation constants and valences for channel block by polyamines. Shown are values of K_d(0 mV) (A) and Z (B) (mean ± SEM; n = 4–6; determined from the fits as shown in Figs. 3 and 4) for block of wild-type and various mutant channels by PUT, SPD, or SPM.

tation E224G+E299S lowers both the affinity and the valence more than either single mutation alone, and triple mutation D172N+E224G+E299S reduces them further (data analysis for channels with the triple mutation was as those with the double mutation).

Kinetics of Wild-type and Mutant Channel Block by Polyamines

Figs. 6–8 show a series of analyses through which we determined the rate constants of channel block by SPD and SPM summarized later in Fig. 9. Polyamines block wild-type and mutant channels with different affinity, voltage dependence, and kinetics. Consequently, to obtain resolvable current transients we had to acquire the data using voltage pulses of varying length and various (appropriate) concentrations of blockers. These factors should be kept in mind when comparing the data in Figs. 6 and 7 (also Figs. 13 and 14). For illustration, we show single-exponential fits of current transients of wild-type and three mutant channels elicited by membrane depolarization from 0 to 70 mV in the presence of SPM at three concentrations (Fig. 6; similar data and fits were obtained with SPD, also from E224G+E299S

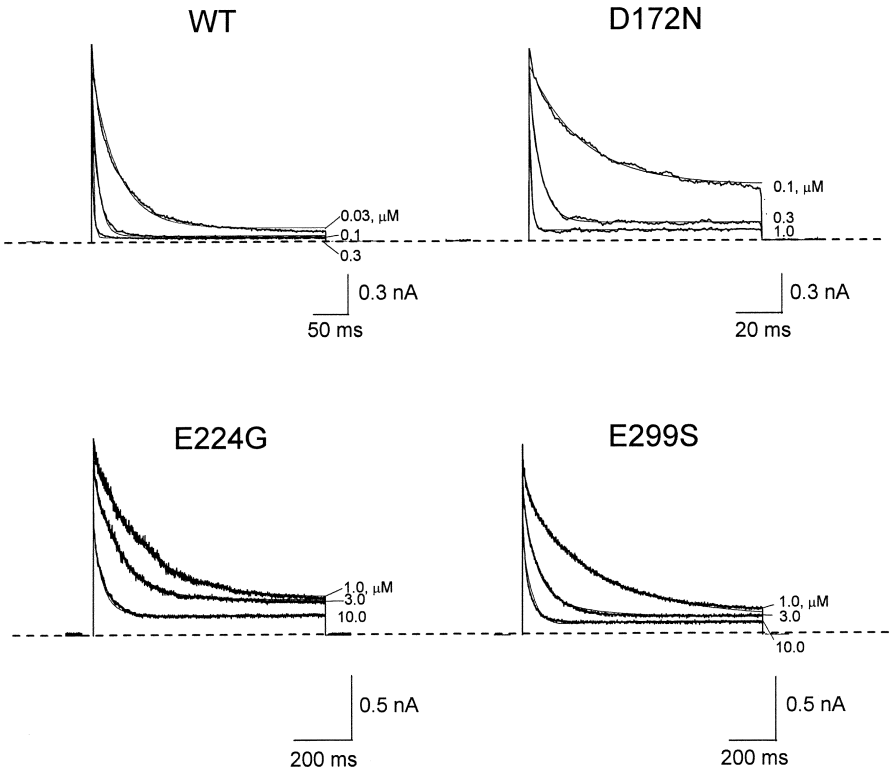

FIGURE 6. Kinetics of voltage jump–induced current relaxations in the presence of spermine. Current traces of wild-type and three mutant channels, each at three appropriate concentrations of SPM, elicited by stepping membrane voltage from 0 to 70 mV. The curves superimposed on the data are single-exponential fits. Dashed lines identify zero current levels.

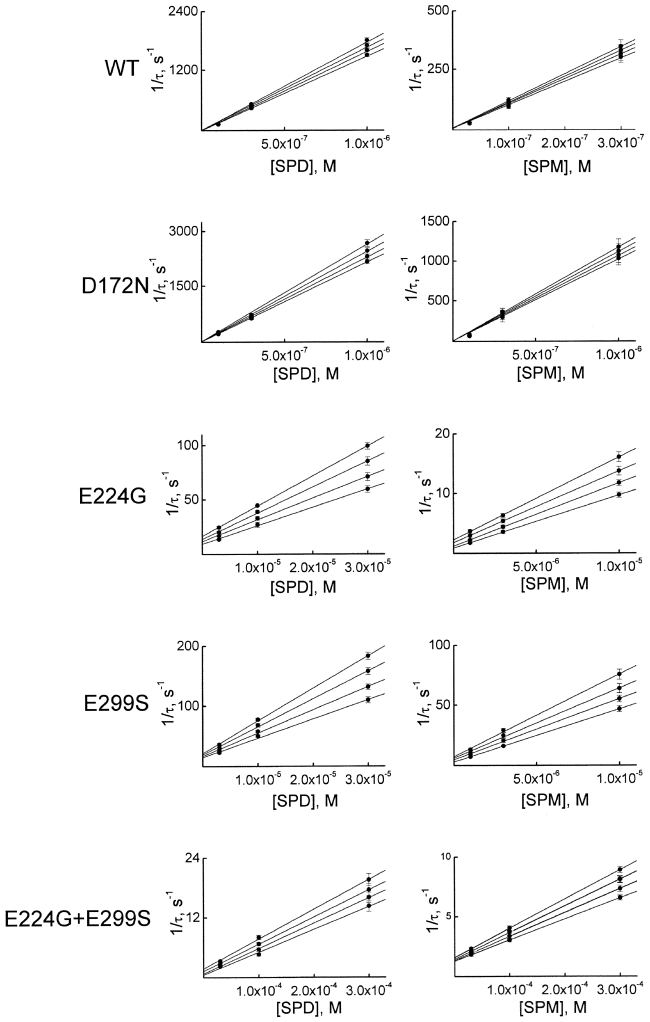

FIGURE 7. Polyamine concentration dependence of the time constant of current transients induced by voltage steps. Reciprocals of the time constants of current transients (mean ± SEM; n = 4–6; obtained from fits such as those shown in Fig. 6) are plotted against the concentration of SPD or SPM for wild-type and several mutant channels. The lines through the data are linear fits. The individual slopes reflect, in ascending order, the kinetics of current transients elicited by stepping membrane voltage from 0 mV to 70, 80, 90, or 100 mV.

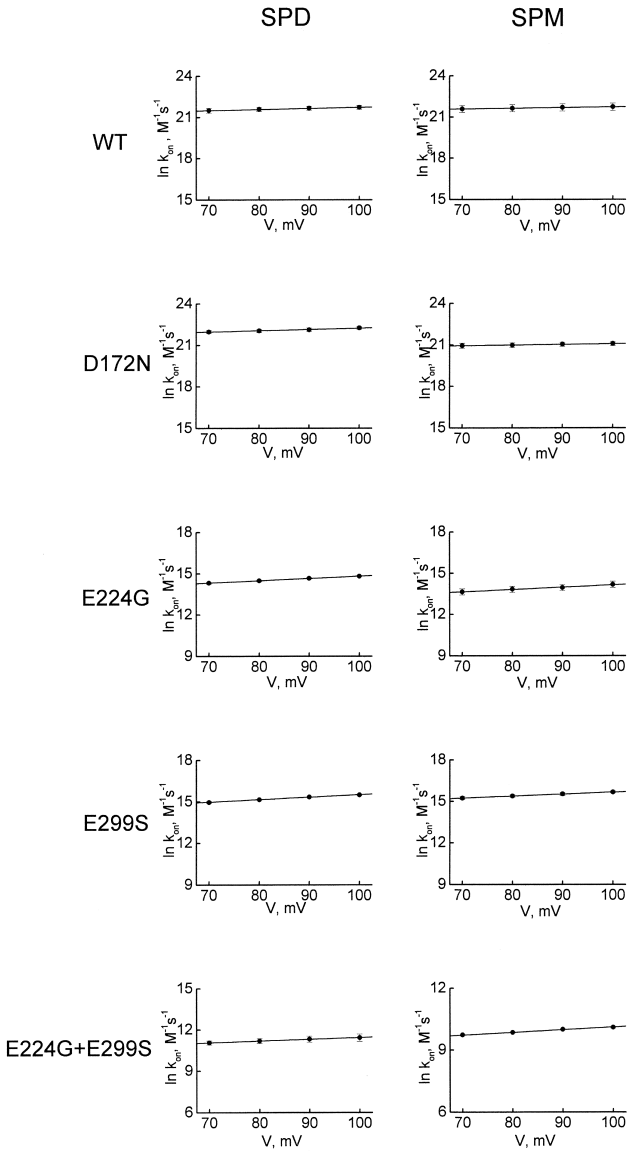

FIGURE 8. Dependence of the rate constant of channel block on membrane voltage. Natural logarithm of the rate constant for formation of the (first) blocked state (k_{on}; mean ± SEM; n = 4–6; determined from the slopes of fits in Fig. 7) is plotted against membrane voltage for wild-type and several mutant channels. The lines through the data represent Boltzmann functions.

double mutant channels). The reciprocal of the time constants from these fits is plotted in Fig. 7 against the concentration of SPD or SPM. The slope of a linear fit to the plots of Fig. 7 gives the rate constant of formation (k_{on}) of the (first) blocked state; its natural logarithm is plotted against membrane voltage in Fig. 8. The lines through the plots in Fig. 8 are fits of Boltzmann functions, yielding k_{on}(0 mV) and the associated valence (z_{on}), which, in turn, are summarized in Fig. 9. The channels containing mutations E224G and/or E299S display a dramatically reduced blocking rate constant for both blockers. The values of z_{on} for all cases are <0.5. As discussed later, there most probably exists more than one blocked state, and thus the interpretation of the Y-intercept in Fig. 7 is not straightforward since it may not simply reflect the unblocking rate constant. Extensive kinetic studies to determine the unblocking rate constant and any additional rate constants for transitions between blocked states, and their voltage dependence, are beyond the scope of this study.

Steady-state Block of Wild-type and Mutant Channels by a Series of Bis-alkyl-amines

We used a series of bis-amines of varying length to help characterize the interactions between the acidic resi-

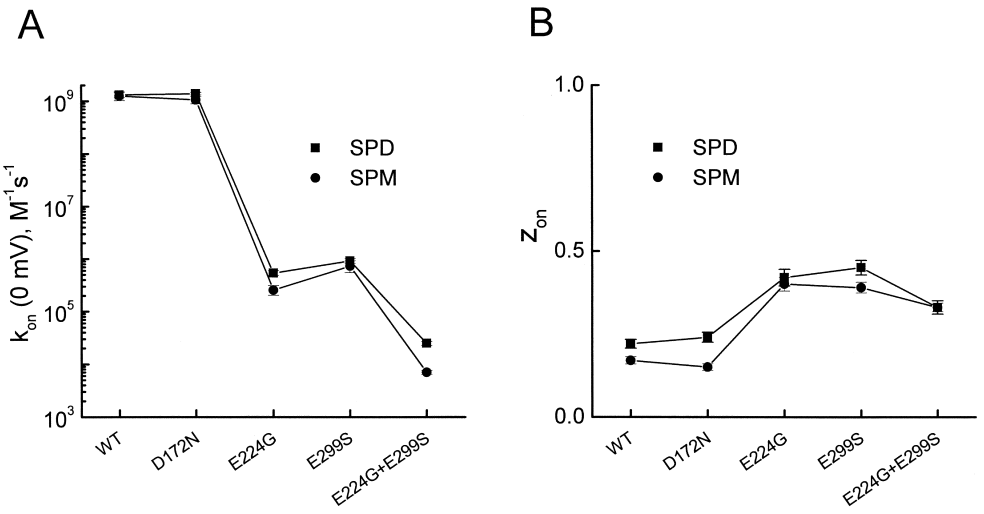

FIGURE 9. Summary of rate constants and valences of channel block by spermidine and spermine. A and B show, respectively, values of k_{on}(0 mV) and z_{on} (mean ± SEM; n = 4–6; determined from fits such as those shown in Fig. 8) for block of wild-type and several mutant channels.

dues in the channel and the amine groups in each natural polyamine species. To that end, we need to know how bis-amines interact with not only D172 (Guo et al., 2003), but also E224 and E299 individually, which for the latter has not been available. For illustration, we show current traces of wild-type and three mutant channels recorded in the absence or presence of bis-C8 (Fig. 10). The fraction of current not blocked by bis-C8 at three appropriate concentrations is plotted against membrane voltage (Fig. 11). The curves through the data are fits performed as described above for the case of PUT (bis-C4; see Fig. 3), which yield K_d(0 mV) and Z. These two fitted parameters are summarized in Fig. 12, not only for bis-C8 but also for the other bis-amines determined in a similar way. The effect of mutation D172N on K_d varies with alkyl chain length, being largest at an intermediate length corresponding to bis-C9, whereas mutations E244G and E299S have comparatively modest, and comparable, effects on bis-amine affinity, independent of their length. As to the valence of channel block, it increases with alkyl chain length in both wild-type and all three single mutant channels in increments of ~1, although the mutations evidently decrease the maximal valence at long chain length. The mutation-induced valence reduction most probably reflects lower occupancy of the inner pore by K^+ ions, although occupancy of the innermost part of the pore may be unaffected since the valence of shorter amines is practically unchanged. However, the effect of multiple mutations appears more far-reaching, as shown with bis-C4 (PUT) in Fig. 5 B.

Kinetics of Wild-type and Mutant Channel Block by Bis-alkyl-amines

Fig. 13 shows current transients in wild-type and three mutant channels elicited by membrane depolarization from 0 to 70 mV in the presence of bis-C8 at three appropriate concentrations. The curves superimposed on the traces are single-exponential fits. The reciprocal of the time constants from these fits is plotted in Fig. 14 against the concentration of bis-C8. The slope of a linear fit to the plots of Fig. 14 gives k_{on}; its natural logarithm is plotted against membrane voltage in Fig. 15. The lines through the plots in Fig. 15 are fits of Boltzmann functions, yielding k_{on}(0 mV) and the associated valence (z_{on}). Similar data and fits were obtained with additional four bis-amines of varying lengths whose blocking kinetics, over practical ranges of membrane voltage and blocker concentration, is sufficiently slow to permit quantitative analysis. Values of k_{on}(0 mV) and z_{on} for all five bis-amines are summarized in Fig. 16. As in the case of polyamine block, mutations E224G and E299S, unlike D172, dramatically lower k_{on}(0 mV) of bis-amines, while z_{on} is generally <0.5 for block by bis-amines of both the wild-type and the three mutant channels.

Thermodynamic Cycle Analysis

We examined interaction energetics of each of three natural polyamines (PUT, SPD, and SPM) with each of the three acidic residues (D172, E224, and E299) in the channel, with respect to each of the eight bis-amines of varying length described above. To do so, we computed the energetic coupling coefficient, Ω (Hidalgo and MacKinnon, 1995), using K_ds (0 mV) of the wild-type and a mutant channel for a polyamine (PM) and for a given bis-amine (Cn) [$\Omega = ({}^{wt}K_d{}^{PM} \times {}^{mt}K_d{}^{bis\text{-}Cn})/({}^{mt}K_d{}^{PM} \times {}^{wt}K_d{}^{bis\text{-}Cn})$]. The results are presented in terms of "RT ln Ω", i.e., the free energy difference between the interaction of a given natural amine blocker with a particular channel residue and the interaction of a given bis-amine with that same residue. For presentation pur-

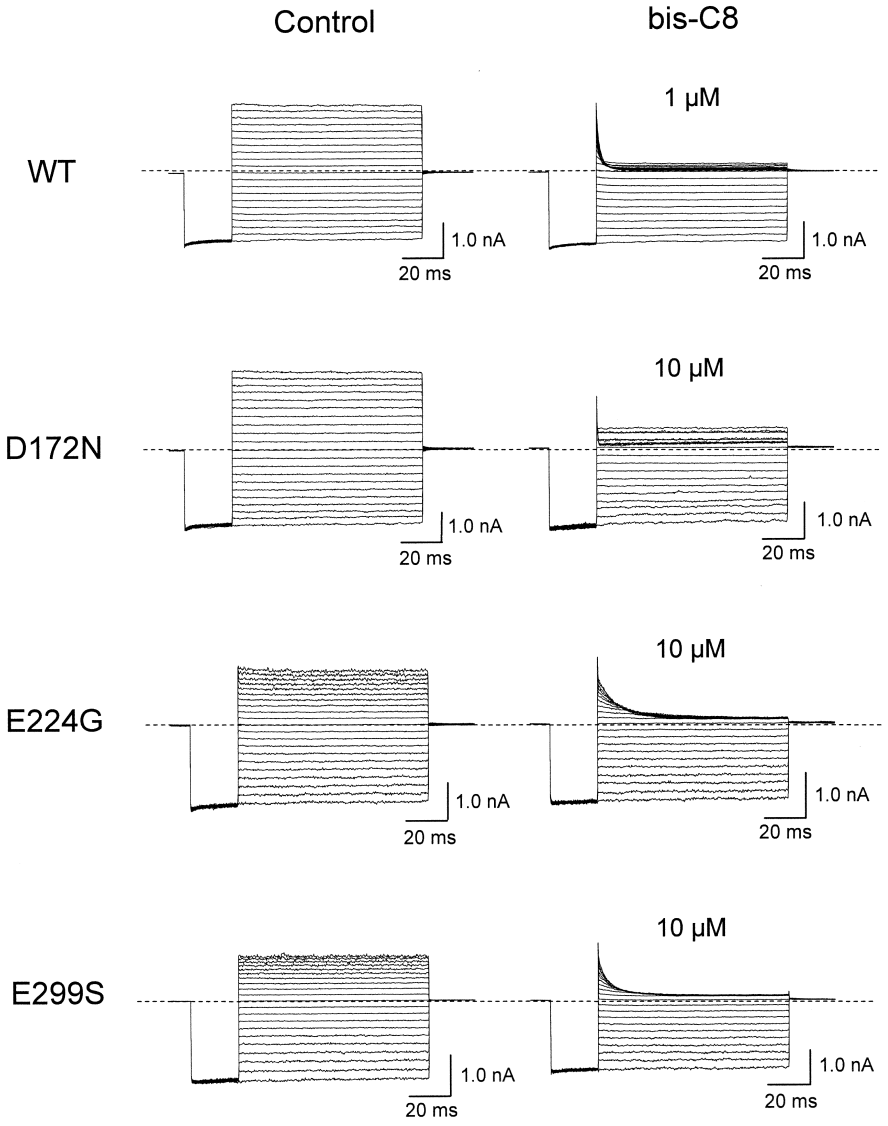

FIGURE 10. Effects of mutations on current inhibition by octamethylene-bis-amine. Shown are currents of wild-type and mutant channels containing a single mutation D172N, E224G, or E299S recorded in the absence (control) or presence of bis-C8 at the concentrations indicated. Dashed lines identify zero current levels.

poses, we will refer to quantity "RT ln Ω" as the interaction energy, whose value is negative, zero, or positive, depending on whether the natural amine interacts with a given residue more, equally, or less strongly than the comparison bis-amine. Fig. 17 A shows the interaction energy for PUT relative to the eight bis-amines. When tested against D172N, the energy value rises from near zero to 1.5 kcal/mol at bis-C9 and then falls with further lengthening bis-amine chain. Its generally positive values indicate that PUT interacts less strongly with D172 than longer bis-amines. In contrast, when tested against E224G or E299S, the energy value is near zero relative to all bis-amines, which indicates that PUT and all bis-amines behave almost equally in their interaction with either residue. As to the interaction energy of SPD relative to bis-amines, when tested against D172N, the energy value increases with increasing alkyl chain length from negative to near zero for bis-C9, and then decreases again at greater lengths (Fig. 17 B). This result indicates that SPD and bis-C9 have comparable energetic interactions with D172. As expected, when tested against E224G or E299S, the energy value is around zero independent of alkyl chain length, suggesting that SPD and the tested bis-amines have comparable energetic interactions with E224 or S299. Finally, we computed the interaction energy for SPM relative to bis-amines (Fig. 17 C). When tested against D172N, all energy values are negative, indicating that SPM interacts more strongly with D172 than any of the tested bis-amines does. The value relative to bis-C4 is −2.8 kcal/mol, giving a lower limit for the interaction energy between D172 and SPM (considering there is finite interaction energy between D172 and bis-C4). On the other hand, the peak value (−1.3 kcal/mole) at bis-C9 represents the difference in interaction energy between D172 with SPM and D172 with bis-C9 whose leading

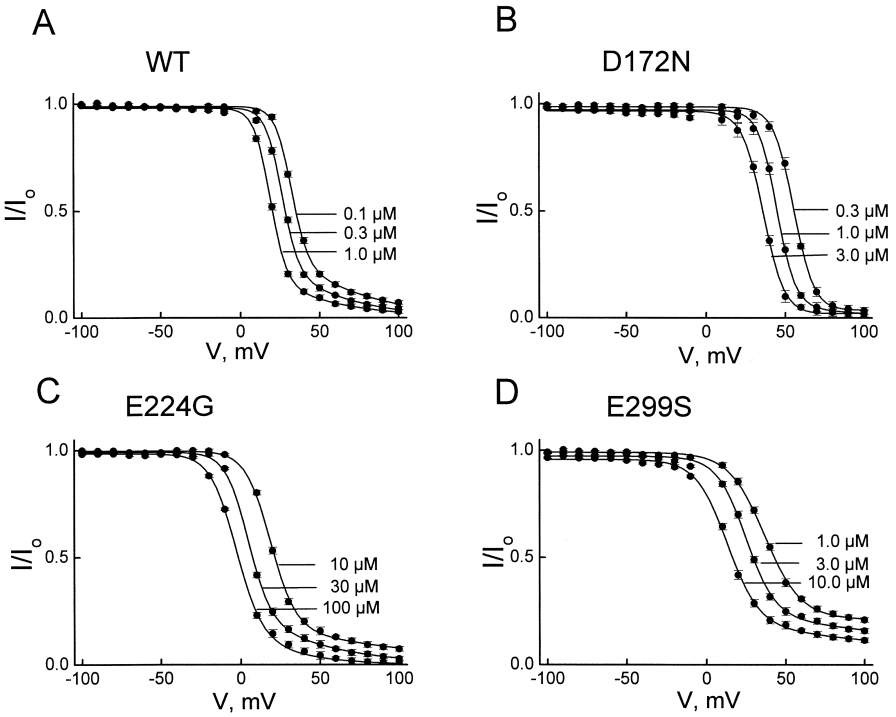

FIGURE 11. Effects of mutations on voltage-dependent block of IRK1 current by octomethylene-bis-amine. The fraction of wild-type and mutant channel currents (mean ± SEM; n = 4–6) not blocked by bis-C8 (at the concentrations indicated) is plotted against membrane voltage. The curves superimposed on the data are fits as described for the case of PUT in RESULTS.

amine is closest to D172. Surprisingly, when tested against E224G or E299S, the values are also negative, instead of around zero, with respect to all bis-amines, indicating that SPM also interacts more strongly with E224 or E299 than any of the bis-amines.

DISCUSSION

As in other K^+ channels, the external, narrow, and K^+-selective part of the ion conduction pore in Kir is formed by the signature sequence between M1 and M2, and a wider part immediately internal to it is lined by M2, which is further extended intracellularly by a structure formed by the COOH terminus (Nishida and MacKinnon, 2002; Kuo et al., 2003). Exposing the intracellular end of the pore to long organic amines causes channel block. In the case of block by alkyl-bis-amines, the trailing amine group of the blocker binds at a more internal site, while the leading one penetrates deeper into the pore toward the ion selectivity filter. This conclusion is based on how interaction energy between certain acidic residues in IRK1 and bis-amine blockers varies with the latter's length (Guo et al., 2003). The interaction energy between D172 and bis-amines of varying length remains minimal for chain lengths up to C6, but rises with further lengthening to a peak at bis-C9, followed by a decrease. These findings are consistent with the view that the leading amine of bis-C9 approaches D172 most closely, while that of bis-C8 or bis-C10 falls slightly short of, or possibly overshoots, D172 (addition-

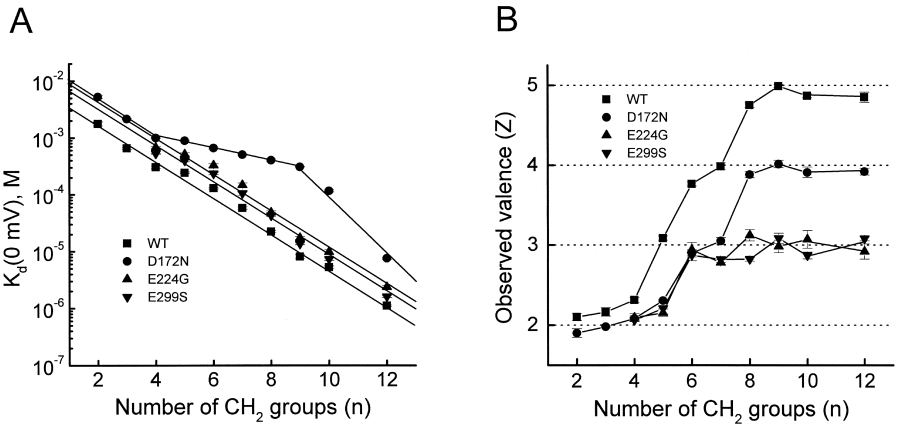

FIGURE 12. Summary of dissociation constants and valences for steady-state channel block by alkyl-bis-amines. Shown in A and B are values of K_d(0 mV) and Z, respectively (mean ± SEM; n = 4–6; determined from fits as shown in Fig. 11), for block of wild-type and three single mutant channels by a series of bis-amines of varying chain length. Bis-C11 is not available commercially.

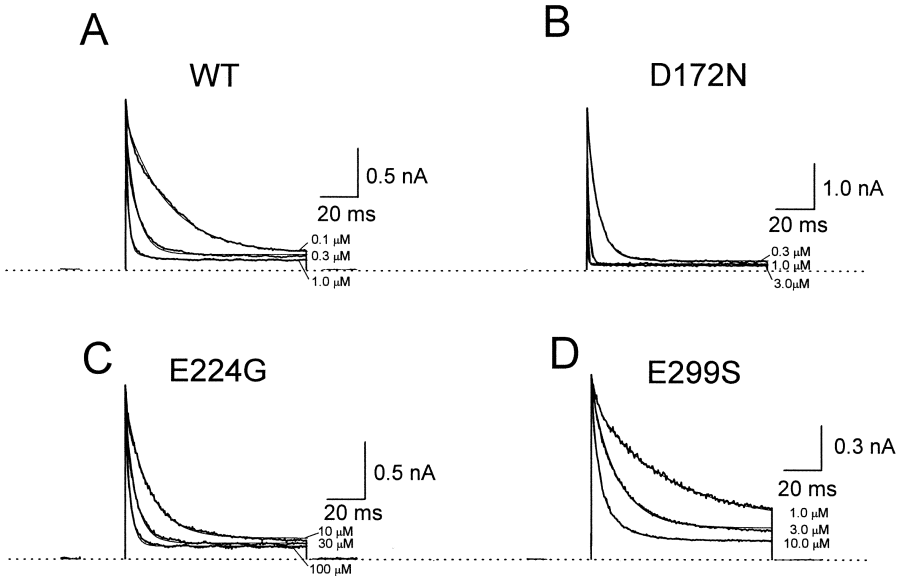

FIGURE 13. Kinetics of voltage jump–induced current relaxations in the presence of octamethylene-bis-amine. Current traces of wild-type and three mutant channels at three concentrations of bis-C8 elicited by stepping membrane voltage from 0 to 70 mV. The curves superimposed on the data are single-exponential fits. Dashed lines identify zero current levels.

ally or alternatively, the drop-off in the "RT ln Ω" value may reflect buckling of the alkyl chain). Thus, with increasing chain length, the leading amine of bis-amines reaches further in the outward direction and encounters an increasing electrostatic potential from D172, whereas the trailing amine remains near the same more internal site and encounters little potential from D172. Supporting the latter conclusion, short and long bis-amines interact equally with the more internally located E224 and E299 residues.

The distance between the residues in the closed-state structure of KirBac1.1 that correspond to D172 and E224/E299 in IRK1, is ~35 Å (Kuo et al., 2003), far greater than the length of bis-C9. If this distance persists in the open state of IRK1, the trailing amine must interact with E224 and E299 over a significant distance, since the leading amine group in bis-C9 is located near the plane of D172. Consistent with this, replacing both residues with neutral ones has only a modest energetic effect on the binding of bis-amines (~0.7 kcal/mol at 0 mV), whereas it dramatically reduces the rate constant of channel block and renders the I-V curve inwardly

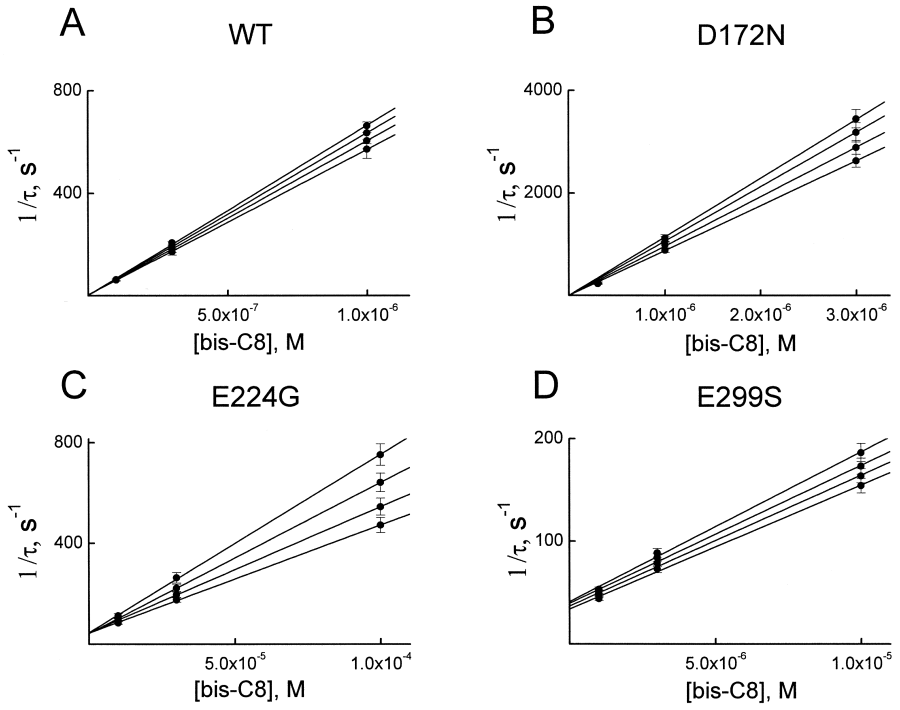

FIGURE 14. Octamethylene-bis-amine concentration dependence of the time constant of current transients induced by voltage steps. Reciprocals of the time constants of current transients (mean ± SEM; n = 4–6; obtained from fits such as those shown in Fig. 13) are plotted against the concentration of bis-C8 for wild-type and three mutant channels. The lines through the data are linear fits. The individual slopes reflect, in ascending order, the kinetics of current transients elicited by stepping membrane voltage from 0 to 70, 80, 90, or 100 mV.

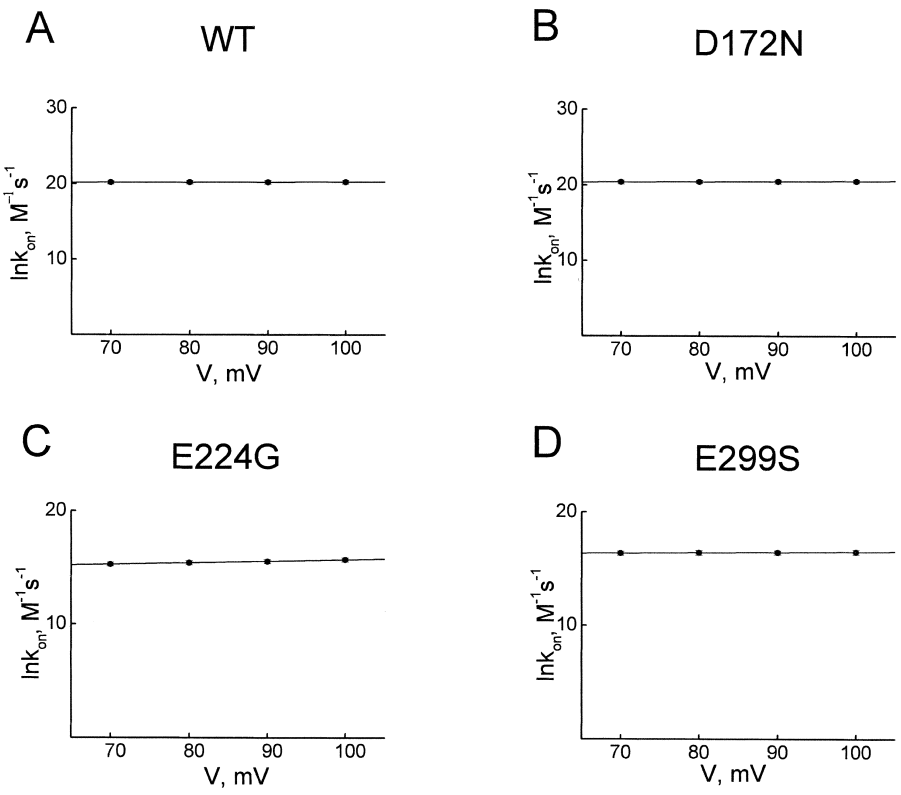

FIGURE 15. Dependence of the rate constant of channel block by octamethylene-bis-amine on membrane voltage. Natural logarithm of the rate constant for formation of the (first) blocked state (k_{on}; mean ± SEM; n = 4–6; determined from the slopes of fits in Fig. 14) is plotted against membrane voltage for wild-type and three mutant channels. The lines through the data represent Boltzmann functions.

rectifying even in the absence of blockers (Guo et al., 2003). In contrast, the electrostatic effect of D172 on the binding of cationic blockers appears more localized (Guo et al., 2003). First, although an acidic residue substituted at various sites in M2 is effective, the substitution must be made within a small region. Second, substituting a neutral residue for D172 neither reduces the apparent rate constant of channel block nor renders the I-V curve inwardly rectifying in the absence of blockers (Guo and Lu, 2002). Third, the interaction energy between D172 and the leading amine group in bis-amines increases steeply (~1.5 kcal/mole) when the alkyl chain is lengthened by only three additional methylene groups (see also Fig. 17). The extent of electrostatic energy change with distance is consistent with the case where the dielectric constant for the region around D172 is lower than that for the bulk solution.

The apparent voltage dependence of steady-state block of Kir channels primarily results from the blocker displacement of K^+ ions across the transmembrane electric field along the pore (Spassova and Lu, 1998, 1999; Guo et al., 2003). With increasing chain length, more K^+ ions are displaced, producing stronger voltage dependence of the apparent affinity with a valence up to approximately five (Guo et al., 2003; Figs. 5 B and 12 B). However, the valence associated with the rate con-

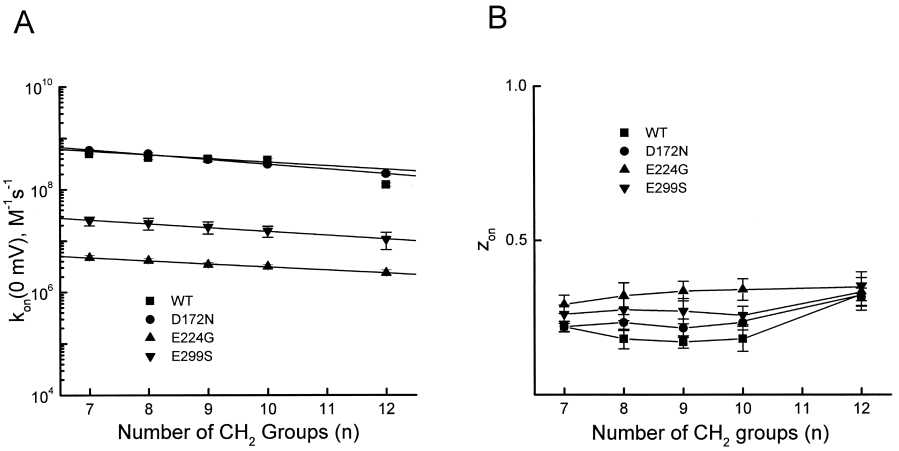

FIGURE 16. Summary of rate constants and valences of channel block by alkyl-bis-amines. Values of k_{on}(0 mV) and z_{on} (mean ± SEM; n = 4–6; determined from fits such as those shown for bis-C8 in Fig. 15) for block of wild-type and three mutant channels are plotted in A and B, respectively.

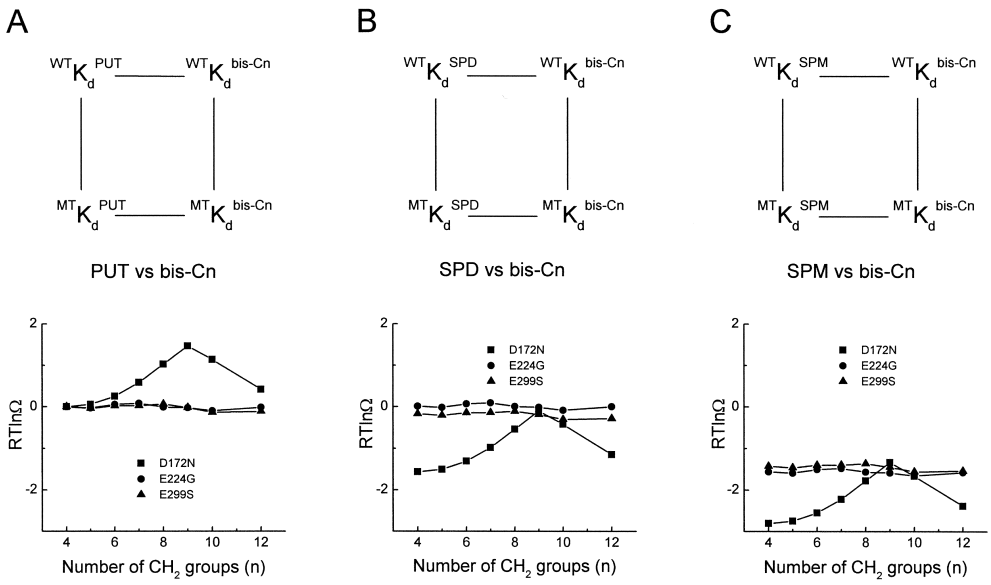

FIGURE 17. Thermodynamic cycle analyses. The four corners are K_ds (0 mV) of the wild-type and a mutant channel for a polyamine (PM) and for a bis-amine (bis-Cn). $\Omega = ({}^{wt}K_d^{PM} \times {}^{mt}K_d^{bis\text{-}Cn})/({}^{mt}K_d^{PM} \times {}^{wt}K_d^{bis\text{-}Cn})$, where K_ds (all at 0 mV) are taken from Figs. 5 A and 12 A. The results are plotted as "RT ln Ω". Shown in A, B, or C are "RT ln Ω" values computed for PUT, SPD, or SPM, with respect to a series of bis-amines of varying length. Each panel shows values computed for each of the three mutant channels (D172N, E224G, and E229S).

stant of current inhibition is <1 for all examined amine blockers in both wild-type and mutant channels (Guo et al., 2003; Figs. 9 B and 16 B). These observations indicate that the ion conduction pore becomes nonconductive (i.e., is "blocked') as soon as an amine blocker approaches the innermost K^+ ion, before reaching its final destination. Thus, there must be two (or more) blocked states (Fig. 18 C).

Knowing how bis-amines interact energetically with the channel helps in understanding the interaction mechanism in the case of natural polyamines. The comparison is in fact directly applicable to PUT, which itself is bis-C4. Since the leading amine group of PUT is energetically less coupled to D172 than that of longer bis-amines, the interaction energy between D172 and PUT (relative to the other bis-amines) is ≥0. With increasing length of the comparison bis-amine, the energy increases from near zero to a peak of ~1.5 kcal/mol at bis-C9 and then decreases with further lengthening. In contrast, since the trailing amine group in all amine blockers binds near the same internal site, the energy for interacting with the more internally located E224 and E299 residues is uniformly near zero, independent of the comparison bis-amine's length.

To acquire stronger voltage dependence by displacing more K^+ ions, a blocker needs to be lengthened to at least the size of bis-C8. Cells evidently do not synthesize bis-C8 simply by extending PUT's methylene chain, but instead generate SPD by attaching an amino-propyl group to PUT. SPD has essentially the same length as bis-C8, but carries an extra amine group in the middle, with noticeable energetic consequences. Since SPD interacts more strongly with D172 than shorter bis-amines, the interaction energy between D172 and SPD (relative to bis-amines) increases with alkyl chain length from negative to near zero at bis-C9, and then decreases as chain length is increased further (Fig. 17 B). The fact that the energy value reaches zero at bis-C9, which is longer, and not at bis-C8, which has the same length as SPD, suggests that besides the leading amine, the middle amine also interacts with D172. This additional interaction raises the total interaction energy of SPD with D172 to that of bis-C9, even though the leading amine in SPD may not approach D172 quite as closely as that in Bis-C9 (Fig. 18 B). The trailing amine in SPD still appears located near the same site as those in bis-amines, since the interaction energy between E224 or E299 and SPD (relative to bis-amines) remains near zero. One reason why the middle amine exhibits significant interactions with D172, but not with E224 or E299 may be that the latter are further away from the middle amine group, and possibly located in a higher dielectric environment more similar to that of the bulk solution.

The pKa of one of the amine groups in SPD is reduced from ~11 to ~8, due to electrostatic repulsion between positively charged amine groups (Palmer and Powell, 1974). The perturbation most probably occurs at the middle amine. Previously, we found that deprotonation of the low-pKa amine group reduces the affinity of SPD (Guo and Lu, 2000b). A plot of wild-type channel current not blocked versus membrane voltage in the presence of a mixture of fully and partially protonated SPD exhibits two descending phases with an intervening hump (Fig. 3). Since the middle amine in SPD interacts with D172 in the channel, mutation D172N that disrupts this interaction should make channel block by fully and partially protonated SPD indistinguishable, i.e., it should eliminate the multiple phases in the blocking curve. Furthermore, the blocking curve

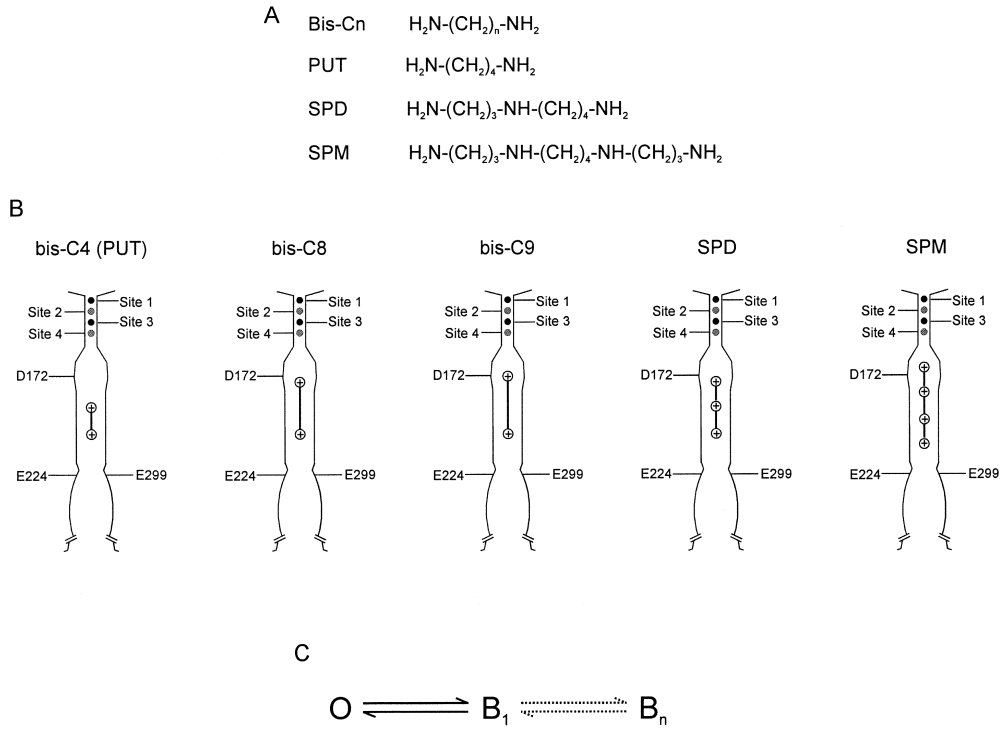

FIGURE 18. Blocker structures, models for blocker-bound channels, and blocking reaction scheme. (A) Chemical structures of bis-Cn, PUT (bis-C4), SPD, and SPM. (B) Models for channel block by bis- and polyamines. K^+ ions present in the blocked inner pores are not drawn. (C) A kinetic model of channel block with one open (O) and n blocked states (B_1...B_n).

for bis-C8, which lacks a middle amine group, should not be multiphasic. Both expectations are verified (Figs. 3 and 11).

SPD, as well as bis-C8 and bis-C9, while sufficiently long to displace the maximal number of K^+ ions and hence exhibit maximal voltage dependence, all bind to the pore with significantly lower affinity than the longer bis-C12 (Figs. 5 A and 12 A). Bis-C12's leading amine may extend outwardly beyond D172, and thus interact electrostatically with it less strongly than that of shorter C9. Despite this, extra hydrophobic interactions between the three additional methylene groups in bis-C12 and the pore overcompensate the reduced electrostatic interactions, resulting in even higher affinity. Cells, again, do not synthesize bis-C12 but, instead, generate SPM by attaching another amino-propyl group to SPD. SPM has essentially the same length as bis-C12, but carries two extra amine groups in the middle. It blocks the channel with even higher affinity than bis-C12. SPM appears to accomplish this in the following way: Two amine groups in one half of the molecule interact primarily with D172, whereas the two in the other half interact primarily with E224 and E299. This binding scheme predicts the following. Interactions of SPM with D172, or with E224 and E229, should be much stronger than those of any bis-amine. Indeed, the electrostatic interaction energy between D172 and the charges in the leading part of SPM amounts to ~3.5 kcal/mol (Fig. 5 A), or 60% more than the ~2.2 kcal/mol between D172 and the leading amine group in bis-C9 (Fig. 12 A) (interaction energy in these and the following two cases was calculated directly from relevant mutation-caused reductions in K_d). Similarly, the electrostatic interaction energy between E224 and E299 and the charges in the trailing part of SPM is ~2.7 kcal/mol (Fig. 5 A) versus ~0.7 kcal/mol for the interaction of E224 and E299 with the trailing amine group in bis-amines (Guo et al., 2003). Effectively, each half of a SPM molecule acts as a pseudo-divalent cation, enhancing the electrostatic interaction and thus the total interaction energy. Therefore, counterintuitively, multiple amines in spermine serve to primarily increase not the voltage dependence, but the affinity of channel block.

As to the channel side, IRK1 offers a set of four possible D172, one from each of the four subunits, to interact electrostatically with the two amine groups in the leading half of a SPM molecule. The amine groups in the trailing half interact with the acidic residues in the COOH terminus over a greater distance and possibly in a higher dielectric environment, and the interactions are therefore not as strong. However, the presence of dual sets of COOH-terminal acidic residues, E224 and E299, apparently help compensate for those attenuating factors. The two sets of COOH-terminal residues, whose counterparts in GIRK1 and KirBac1.1 channels form a ring (Nishida and MacKinnon, 2002; Kuo et al., 2003), interact with the blocker in an energetically comparable manner (Fig. 5 A). Besides their energetic effects, E224 and E299 also help maximize the rate constant of channel block by polyamines (Figs. 9 A and 16 A). Additionally, replacement of the acidic residues by

neutral ones reduces the apparent valence of channel block (Figs. 5 B and 12 B). This finding strongly implies that their presence enhances K^+ occupancy of the inner pore and therefore the number of moving charges coupled to the binding-unbinding of a long blocker, producing the observed strong voltage dependence. Without the three sets of acidic residues, an IRK1 pore loses its most characteristic property that distinguishes it from other types of K^+ channels, i.e., the exceedingly high affinity and strong voltage dependence of its block by intracellular long polyamines (Figs. 5 and 12). Evidently, through evolution, nature has optimized both IRK1 and SPM to practical perfection for producing rapid, high-affinity, and strongly voltage-dependent block, manifested as remarkably sharp rectification, which allows the generation of the plateau phase and helps accelerate the descending phase in the cardiac action potential (Noble, 1962, 1965; Zaritsky et al., 2001).

We thank P. De Weer for critical review of our manuscript, L.Y. Jan for IRK1 cDNA, J. Yang for IRK1 cDNA subcloned in the pGEM-HESS vector.

This study was supported by NIH grant GM55560. Z. Lu was the recipient of an Independent Scientist Award from the NIH (HL03814).

Olaf S. Andersen served as editor.

Submitted: 19 June 2003
Accepted: 16 September 2003

REFERENCES

Armstrong, C.M., and L. Binstock. 1965. Anomalous rectification in the squid giant axon injected with tetraethylammonium chloride. *J. Gen. Physiol.* 48:859–872.

Bianchi, L., M.L. Roy, M. Taglialatela, D.W. Lundgren, A.M. Brown, and E. Ficker. 1996. Regulation by spermine of native inward rectifier K^+ channels in RBL-1 cells. *J. Biol. Chem.* 271:6114–6121.

Doyle, D.A., C.J. Morais, R.A. Pfuetzner, A. Kuo, J.M. Gulbis, S.L. Cohen, B.T. Chait, and R. MacKinnon. 1998. The structure of the potassium channel: molecular basis of K^+ conduction and selectivity. *Science.* 280:69–77.

Fakler, B., U. Brandle, E. Glowatzki, S. Weidemann, H.P. Zenner, and J.P. Ruppersberg. 1995. Strong voltage-dependent inward rectification of inward rectifier K^+ channels is caused by intracellular spermine. *Cell.* 80:149–154.

Ficker, E., M. Taglialatela, B.A. Wible, C.M. Henley, and A.M. Brown. 1994. Spermine and spermidine as gating molecules for inward rectifier K^+ channels. *Science.* 266:1068–1072.

Guo, D., and Z. Lu. 2000a. Mechanism of cGMP-gated channel block by intracellular polyamines. *J. Gen. Physiol.* 115:783–797.

Guo, D., and Z. Lu. 2000b. Mechanism of IRK1 channel block by intracellular polyamines. *J. Gen. Physiol.* 115:799–813.

Guo, D., and Z. Lu. 2000c. Pore block versus intrinsic gating in the mechanism of inward rectification in the strongly-rectifying IRK1 channel. *J. Gen. Physiol.* 116:561–568.

Guo, D., and Z. Lu. 2002. IRK1 inward rectifier K^+ channels exhibit no intrinsic rectification. *J. Gen. Physiol.* 120:539–551.

Guo, D., Y. Ramu, A.M. Klem, and Z. Lu. 2003. Mechanism of rectification in inward-rectifier K^+ channels. *J. Gen. Physiol.* 121:261–275.

Hagiwara, S., S. Miyazaki, and N.P. Rosenthal. 1976. Potassium current and the effect of cesium on this current during anomalous rectification of the egg cell membrane of a starfish. *J. Gen. Physiol.* 67:621–638.

Hagiwara, S., and K. Takahashi. 1974. The anomalous rectification and cation selectivity of the membrane of a starfish egg cell. *J. Membr. Biol.* 18:61–80.

Hidalgo, P., and R. MacKinnon. 1995. Revealing the architecture of a K^+ channel pore through mutant cycles with a peptide inhibitor. *Science.* 268:307–310.

Ho, K., C.G. Nichols, W.J. Lederer, J. Lytton, P.M. Vassilev, M.V. Kanazirska, and S.C. Hebert. 1993. Cloning and expression of an inwardly rectifying ATP-regulated potassium channel. *Nature.* 362:31–38.

Hodgkin, A.L., and P. Horowicz. 1959. The influence of potassium and chloride ions on the membrane potential of single muscle fibres. *J. Physiol.* 148:127–160.

Ishihara, K., A. Mitsuiye, A. Noma, and M. Takano. 1989. The Mg^{2+} block and intrinsic gating underlying inward rectification of the K^+ current in guinea-pig cardiac myocytes. *J. Physiol.* 419:297–320.

Katz, B. 1949. Les constantes électriques de la membrane du muscle. *Arch. Sci. Physiol. (Paris).* 3:285–299.

Kubo, Y., and Y. Murata. 2001. Control of rectification and permeation by two distinct sites after the second transmembrane region in Kir2.1 K^+ channel. *J. Physiol.* 531:645–660.

Kubo, Y., T.J. Baldwin, Y.N. Jan, and L.Y. Jan. 1993. Primary structure and functional expression of a mouse inward rectifier potassium channel. *Nature.* 362:127–133.

Kuo, A., J.M. Gulbis, J.F. Antcliff, T. Rahman, E.D. Lowe, J. Zimmer, J. Cuthbertson, F.M. Ashcroft, T. Ezaki, and D.A. Doyle. 2003. Crystal structure of the potassium channel KirBac1.1 in the closed state. *Science.* 300:1922–1926.

Kurachi, Y. 1985. Voltage-dependent activation of the inward-rectifier potassium channel in the ventricular cell membrane of guinea-pig heart. *J. Physiol.* 366:365–385.

Liman, E.R., J. Tytgat, and P. Hess. 1992. Subunit stoichiometry of a mammilian K^+ channel determined by construction of multimeric cDNAs. *Neuron.* 9:861–871.

Lopatin, A.N., E.N. Makhina, and C.G. Nichols. 1994. Potassium channel block by cytoplasmic polyamines as the mechanism of intrinsic rectification. *Nature.* 372:366–369.

Lopatin, A.N., L.M. Shantz, C.A. Mackintosh, and C.G. Nichols. 2000. Modulation of potassium channels in the hearts of transgenic and mutant mice with altered polyamine biosynthesis. *J. Mol. Cell. Cardiol.* 32:2007–2024.

Lu, Z., and R. MacKinnon. 1994. Electrostatic tuning of Mg^{2+} affinity in an inward-rectifier K^+ channel. *Nature.* 371:243–246.

Matsuda, H., A. Saigusa, and H. Irisawa. 1987. Ohmic conductance through the inwardly rectifying K channel and blocking by internal Mg^{2+}. *Nature.* 325:156–159.

Morais-Cabral, J.H., Y. Zhou, and R. MacKinnon. 2001. Energetic optimization of ion conduction rate by the K^+ selectivity filter. *Nature.* 414:37–42.

Nishida, M., and R. MacKinnon. 2002. Structural basis of inward rectification: Cytoplasmic pore of the G protein-gated inward rectifier GIRK1 at 1.8 Å resolution. *Cell.* 111:957–965.

Noble, D. 1962. A modification of Hodgkin-Huxley equations applicable to Purkinje fibre action and pace-maker potentials. *J. Physiol.* 160:317–352.

Noble, D. 1965. Electrical properties of cardiac muscle attributable to inward going (anomalous) rectification. *J. Cell. Comp. Physiol.* 66:127–136.

Palmer, B.N., and H.K.J. Powell. 1974. Polyamine complexes with seven-membered chelate rings: complex formation of 3-azahep-

tane-1,7-diamine, 4-azaoctane-1,8-diamine (spermidine), and 4,9-diazadodecane-1,12-diamine (spermine) with copper (II) and hydrogen ions in aqueous solution. *J. Chem. Soc. Dalton*. 19:2089–2092.

Shyng, S.L., Q. Sha, T. Ferrigni, A.N. Lopatin, and C.G. Nichols. 1996. Depletion of intracellular polyamines relieves inward rectification of potassium channels. *Proc. Natl. Acad. Sci. USA*. 93: 12014–12019.

Silver, M.R., and T.E. DeCoursey. 1990. Intrinsic gating of inward rectifier in bovine pulmonary artery endothelial cells in the presence and absence of internal Mg^{2+}. *J. Gen. Physiol.* 96:109–133.

Spassova, M., and Z. Lu. 1998. Coupled ion movement underlies rectification in an inward-rectifier K^+ channel. *J. Gen. Physiol.* 112:211–221.

Spassova, M., and Z. Lu. 1999. Tuning the voltage dependence of tetraethylammonium block with permeant ions in an inward-rectifier K^+ channel. *J. Gen. Physiol.* 114:415–426.

Stanfield, P.R., N.W. Davies, P.A. Shelton, I.A. Khan, W. Brammar, N.B. Standen, and E.C. Conley. 1994a. The intrinsic gating of inward rectifier K^+ channels expressed from the murine IRK1 gene depends on voltage, K^+, Mg^{2+}. *J. Physiol.* 475:1–7.

Stanfield, P.R., N.W. Davies, P.A. Shelton, M.J. Sutcliffe, I.A. Khan, W.J. Brammar, N.B. Standen, and E.C. Conley. 1994b. A single aspartate residue is involved in both intrinsic gating and blockage by Mg^{2+} of the inward rectifier, IRK1. *J. Physiol.* 478:1–6.

Taglialatela, M., E. Ficker, B.A. Wible, and A.M. Brown. 1995. C-terminus determinants for Mg^{2+} and polyamine block of the inward rectifier K^+ channel IRK1. *EMBO J.* 14:5532–5541.

Taglialatela, M., B.A. Wible, R. Caporaso, and A.M. Brown. 1994. Specification of pore properties by the carboxyl terminus of inwardly rectifying K^+ channels. *Science*. 264:844–847.

Vandenberg, C.A. 1987. Inward rectification of a potassium channel in cardiac ventricular cells depends on internal magnesium ions. *Proc. Natl. Acad. Sci. USA*. 84:2560–2564.

Wible, B.A., M. Taglialatela, E. Ficker, and A.M. Brown. 1994. Gating of inwardly rectifying K^+ channels localized to a single negatively charged residue. *Nature*. 371:246–249.

Yang, J., Y.N. Jan, and L.Y. Jan. 1995. Control of rectification and permeation by residues in two distinct domains in an inward rectifier K^+ channel. *Neuron*. 14:1047–1054.

Zaritsky, J.J., J.B. Redell, B.L. Tempel, and T.L. Schwarz. 2001. The consequence of disrupting cardiac inwardly rectifying K^+ current (I_{K1}) as revealed by the targeted deletion of the murine *Kir2.1* and *Kir2.2* genes. *J. Physiol.* 533:697–710.

Zhou, Y., J.H. Morais-Cabral, and R. MacKinnon. 2001. Chemistry of ion coordination and hydration revealed by a K^+ channel-Fab complex at 2.0 Å resolution. *Nature*. 414:43–48.